



Marine and Maritime Intelligent Robotics Program M1

Geometric, Kinematic and Dynamical modeling of Robotic systems

Submitted by

MD Ether Deowan
Student ID: 22303698

Tihan Mahmud Hossain
Student ID: 22303703

Submitted to

Cedric Anthierens
University de Toulon

October 30, 2023

Experiment 1 : SCARA ROBOT

1 Frame and DH/Khalil Formalism

The frame of a SCARA robot is typically defined as follows:

Base Frame: The base frame is the robot's fixed or stationary frame of reference. It is usually centered at the robot's mounting point and serves as the origin for the robot's coordinate system. The X and Y axes are typically aligned with the robot's two rotary joints, and the Z-axis is oriented vertically.

Tool Frame: The tool frame is the coordinate system defined at the robot's end-effector . It allows specify the position and orientation of the tool with respect to the robot's base frame. The X, Y, and Z axes of the tool frame are aligned with the tool's orientation.

1.1 SCARA Robot Frame

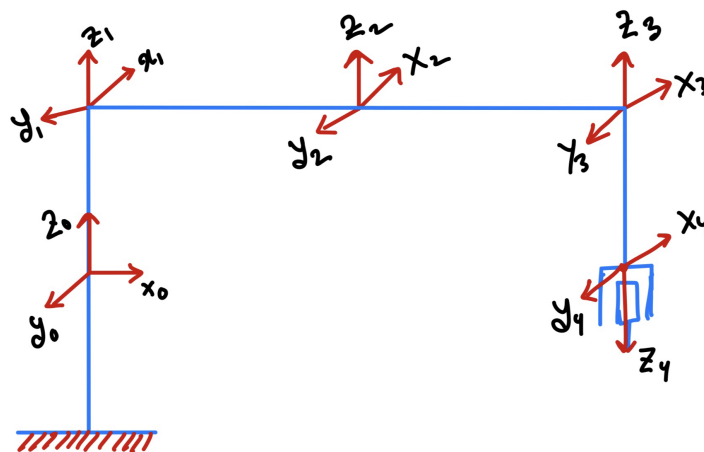


Figure 2: SCARA ROBOT FRAME

1.2 DH parameter

Frame Number	Type of joint σ	Distance along X_{i-1} , d	Angle Around X_{i-1} , α	Distance along Z_{i-1} , r	Angle around Z, ϑ
1	0	0	0	452.4	θ_1
2	0	220	0	0	θ_2
3	0	240	0	0	θ_3
4	1	0	180	452.4-340-R	0

1.3 Homogeneous Transform Matrix

$$T_0^1 = \begin{pmatrix} \cos(\theta_1) & -\sin(\theta_1) & 0 & 0 \\ \sin(\theta_1) & \cos(\theta_1) & 0 & 0 \\ 0 & 0 & 1 & 0 \\ 0 & 0 & 0 & 1 \end{pmatrix}$$

$$T_1^2 = \begin{pmatrix} \cos(\theta_2) & -\sin(\theta_2) & 0 & 220 \\ \sin(\theta_2) & \cos(\theta_2) & 0 & 0 \\ 0 & 1 & 0 & 0 \\ 0 & 0 & 0 & 1 \end{pmatrix}$$

$$T_2^3 = \begin{pmatrix} \cos(\theta_3) & -\sin(\theta_3) & 0 & 240 \\ \sin(\theta_3) & \cos(\theta_3) & 0 & 0 \\ 0 & 0 & 1 & 0 \\ 0 & 0 & 0 & 1 \end{pmatrix}$$

$$T_3^4 = \begin{pmatrix} 1 & 0 & 1 & 0 \\ 0 & 1 & 0 & 1 \\ 0 & 0 & -1 & 452.4 - 340 - R \\ 0 & 0 & 0 & 1 \end{pmatrix}$$

1.4 Homogeneous Transform Matrix for First Two DOF [0-3]

$$T_0^3 = \begin{pmatrix} \cos(\theta_{123}) & -\sin(\theta_{123}) & 0 & 220\cos\theta_1 + 240\cos\theta_{12} \\ \sin(\theta_{123}) & \cos(\theta_{123}) & 0 & 220\sin\theta_1 + 240\sin\theta_{12} \\ 0 & 0 & 1 & 0 \\ 0 & 0 & 0 & 1 \end{pmatrix}$$

1.5 Jacobian of first two dof link

$$J = \begin{pmatrix} -L_1 \sin\theta_1 - L_2 \sin\theta_{12} & -L_2 \sin(\theta_{12}) & 0 \\ L_1 \cos\theta_1 + L_2 \cos\theta_{12} & L_2 \cos(\theta_{12}) & 0 \\ 1 & 1 & 1 \end{pmatrix}$$

1.6 Singularities

Singularities, points in the robot's configuration where its motion becomes limited or unpredictable, are examined. The objective is to provide insights into how these singularities impact the robot's operation, discuss detection and avoidance strategies, and outline potential future work in addressing these challenges.

The determinant of the jacobian is

$$J_{Det} = 52800 \sin(\theta_1 + \theta_2) \cos(\theta_1) - 52800 \cos(\theta_1 + \theta_2) \sin(\theta_1)$$

Therefore,

$$\text{Angle } \theta_1 = 0$$

$$\text{Angle } \theta_2 = 0$$

Singularities in a SCARA robot configuration are identified when the determinant of the Jacobian matrix equals zero. Through mathematical analysis, it has been established that these singularities manifest when the joint angle 'theta' is equal to zero.

Experiment 2 : Hexabot Robot

2 Frame and DH/Khalil Formalism

2.1 Hexabot robot Frame with 3 DOF

In this system it consisting of the leg with three revolute joints hip,knee and ankle with a punctual foot print, has a total of 3 degrees of freedom, Each revolute joint provides one rotational DOF and punctual footprint doesn't provide any additional DOF.

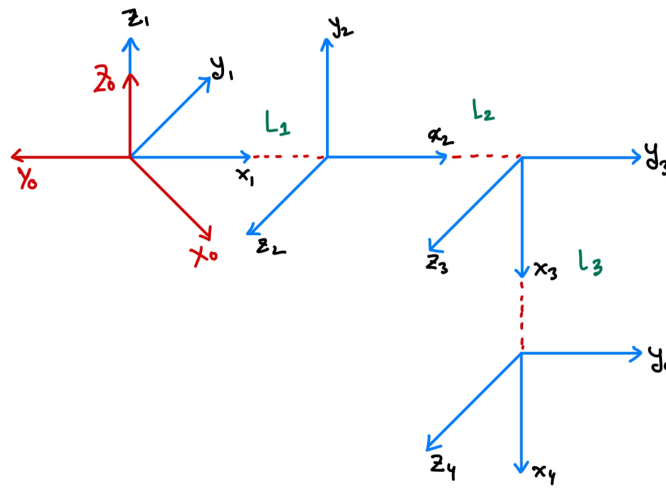


Figure 3: HEXABOT Robot Frame

2.2 DH parameter

$$L_1 = 50mm$$

$$L_2 = 100mm$$

$$L_3 = 100mm$$

Frame Number	Type of joint σ	Distance along X_i, d	Angle Around X_{i-1}, α	Distance along Z_{i-1}, r	Angle around Z, ϑ
1	0	0	0	0	θ_1
2	L_1	90°	0	0	θ_2
3	L_2	0	0	0	θ_3
4	L_3	0	0	0	0

2.3 Homogeneous Transform Matrix

$$T_0^1 = \begin{pmatrix} \cos(\theta_1) & -\sin(\theta_1) & 0 & 0 \\ \sin(\theta_1) & \cos(\theta_1) & 0 & 0 \\ 0 & 0 & 1 & 0 \\ 0 & 0 & 0 & 1 \end{pmatrix}$$

$$T_1^2 = \begin{pmatrix} \cos(\theta_2) & 0 & \sin(\theta_2) & L_1 \\ 0 & 0 & -1 & 0 \\ \sin(\theta_2) & 0 & -\cos(\theta_2) & 0 \\ 0 & 0 & 0 & 1 \end{pmatrix}$$

$$T_2^3 = \begin{pmatrix} \cos(\theta_3) & -\sin(\theta_3) & 0 & L_2 \\ \sin(\theta_3) & \cos(\theta_3) & 0 & 0 \\ 0 & 0 & 1 & 0 \\ 0 & 0 & 0 & 1 \end{pmatrix}$$

$$T_3^4 = \begin{pmatrix} 1 & 0 & 1 & L_3 \\ 0 & 1 & 0 & 1 \\ 0 & 0 & 1 & 0 \\ 0 & 0 & 0 & 1 \end{pmatrix}$$

2.4 Homogeneous Transform Matrix for First Two DOF [0-3]

$$T_0^1 * T_1^2 * T_2^3 * T_3^4 = T_0^4$$

$$T_0^4 = \begin{pmatrix} \cos(\theta_2 - \theta_3) \cdot \cos(\theta_1) & \sin(\theta_2 - \theta_3) \cdot \cos(\theta_1) & \sin(\theta_1) & 50 \cdot \cos(\theta_1) \cdot \sigma_1 \\ \cos(\theta_2 - \theta_3) \cdot \sin(\theta_1) & \sin(\theta_2 - \theta_3) \cdot \sin(\theta_1) & -\cos(\theta_1) & 50 \cdot \sin(\theta_1) \cdot \sigma_1 \\ \sin(\theta_2 + \theta_3) & \cos(\theta_2 + \theta_3) & 0 & 100 \cdot \sin(\theta_2 + \theta_3) + 100 \cdot \sin(\theta_2) \\ 0 & 0 & 0 & 1 \end{pmatrix}$$

where $\sigma_1 = 2 \cdot \cos(\theta_2 - \theta_3) + 2 \cdot \cos(\theta_2) + 1$

2.5 Calculating Jacobian Matrix

2.5.1 Translation Matrix

$$T_{Matrix} = \begin{pmatrix} 50 \cdot \cos(\theta_1) (2 \cos(\theta_2 - \theta_3) + 2 \cdot \cos(\theta_2) + 1) \\ 50 \cdot \sin(\theta_1) (2 \cos(\theta_2 - \theta_3) + 2 \cdot \cos(\theta_2) + 1) \\ 100 \cdot \sin(\theta_2 + \theta_3) + 100 \cdot \sin(\theta_2) \end{pmatrix}$$

2.5.2 Jacobian Matrix

$$\begin{aligned}
j11 &= -50 \sin(\theta_1) (2 \cos(\theta_2 - \theta_3) + 2 \cos(\theta_2) + 1) \\
j12 &= -50 \cos(\theta_1) (2 \sin(\theta_2 - \theta_3) + 2 \sin(\theta_2) + 1) \\
j13 &= 100 \sin(\theta_2 - \theta_3) \cos(\theta_1) \\
j21 &= 50 \cos(\theta_1) (2 \cos(\theta_2 - \theta_3) + 2 \cos(\theta_2) + 1) \\
j22 &= -50 \sin(\theta_1) (2 \sin(\theta_2 - \theta_3) + 2 \sin(\theta_2)) \\
j23 &= 100 \sin(\theta_2 - \theta_3) \sin(\theta_1) \\
j31 &= 0 \\
j32 &= 100 \cos(\theta_2 + \theta_3) + 100 \cos(\theta_2) \\
j33 &= 100 \cos(\theta_2 + \theta_3)
\end{aligned}$$

$$Jacobian = \begin{pmatrix} -50 \sin(\theta_1) \sigma_1 & -50 \cos(\theta_1) \sigma_2 & 100 \sin(\theta_2 - \theta_3) \cos(\theta_1) \\ 50 \cos(\theta_1) \sigma_1 & -50 \sin(\theta_1) \sigma_2 & 100 \sin(\theta_2 - \theta_3) \sin(\theta_1) \\ 0 & 100 \cos(\theta_2 + \theta_3) + 100 \cos(\theta_2) & 100 \cos(\theta_2 + \theta_3) \end{pmatrix}$$

where

$$\begin{aligned}
\sigma_1 &= 2 \cos(\theta_2 - \theta_3) + 2 \cos(\theta_2) + 1 \\
\sigma_2 &= 2 \sin(\theta_2 - \theta_3) + 2 \sin(\theta_2)
\end{aligned}$$

3 Matlab simulation of Hexabot Leg

3.1 Matlab Simulink Frame

The presented figure encapsulates a Simulink model illustrating the kinematic chain of a robotic leg, showcasing the intricate interconnectedness of the leg's components. With a deliberate design, the model delineates the movement of the leg through three pivotal joints: the Hip, Knee, and Ankle. Each joint, featuring a revolute configuration, offers a realistic representation of the leg's motion. The model distinctly incorporates four frames for each solid component, providing a comprehensive geometric description. Frame 0 serves as the stationary base fixed on the robot's body, maintaining a constant reference point. The remaining frames, distributed across the leg's segments, detail the gravity center and the endpoint of each solid body. This model elegantly portrays the dynamics of the leg's movement by elucidating the interconnectedness between the base frame, individual segments, and the distinct joint connections. This structured approach allows for a meticulous understanding of the leg's kinematics, enabling precise simulation and analysis of the leg's motion within a robotics system.

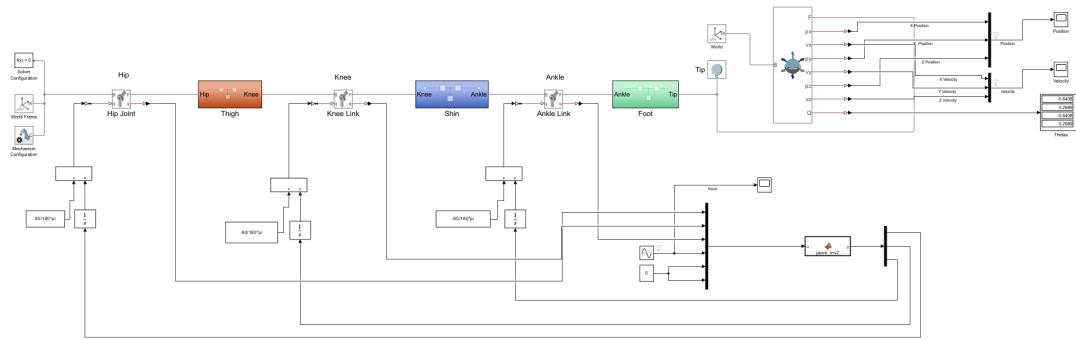


Figure 4: Matlab Simulink Full Model Diagram

3.2 Matlab Simulink Subsystem

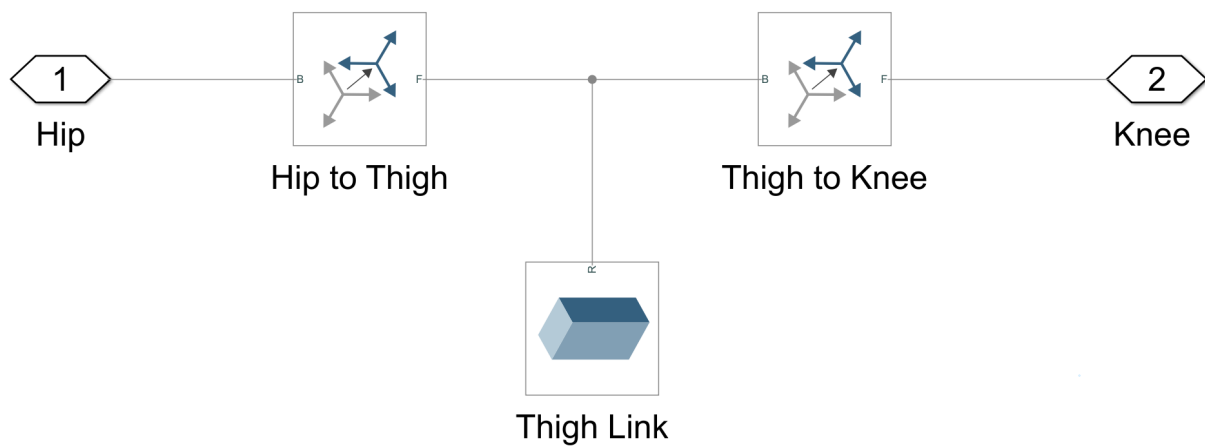


Figure 5: Thigh Subsystem

3.3 Rendering in Mechanics Explorer Window

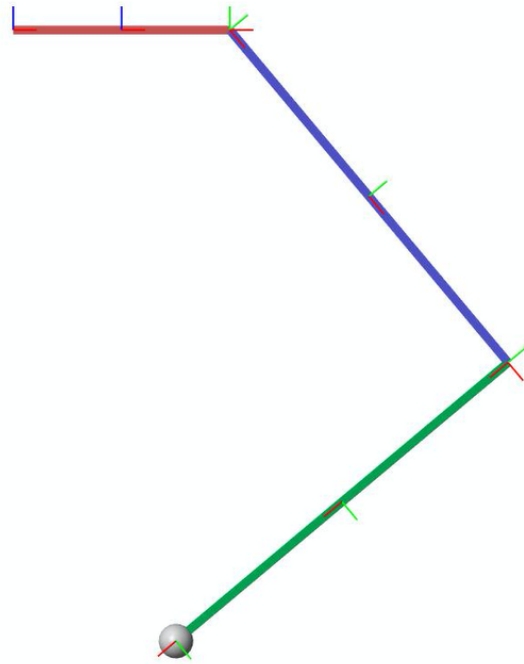


Figure 6: Right View of the Model

Figures 6 and 7 in the Mechanics Explorer Window provide essential perspectives: Figure 6 offers a right-side view, while Figure 7 presents a top-down view of the model. These visuals offer insights into the model's layout and spatial configuration from lateral and overhead angles, aiding in understanding the system's structure and interconnections.

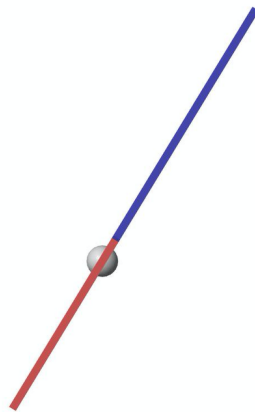


Figure 7: Top View of the Model

3.4 Foot Position

Figure 8 illustrates the trajectory of the foot over time concerning the three axes of the base frame while aiming for a sinusoidal speed specifically along the X-axis. The graph demon-

strates the path followed by the foot in a timeframe concerning the movement along the X, Y, and Z axes of the base frame. The intended motion profile for the foot's movement along the X-axis is sinusoidal, depicting a smooth, repetitive back-and-forth motion. This graphical depiction serves to showcase how the foot trajectory evolves over time, providing a clear understanding of the leg's movement in a specific direction while considering the dynamics along different spatial axes.

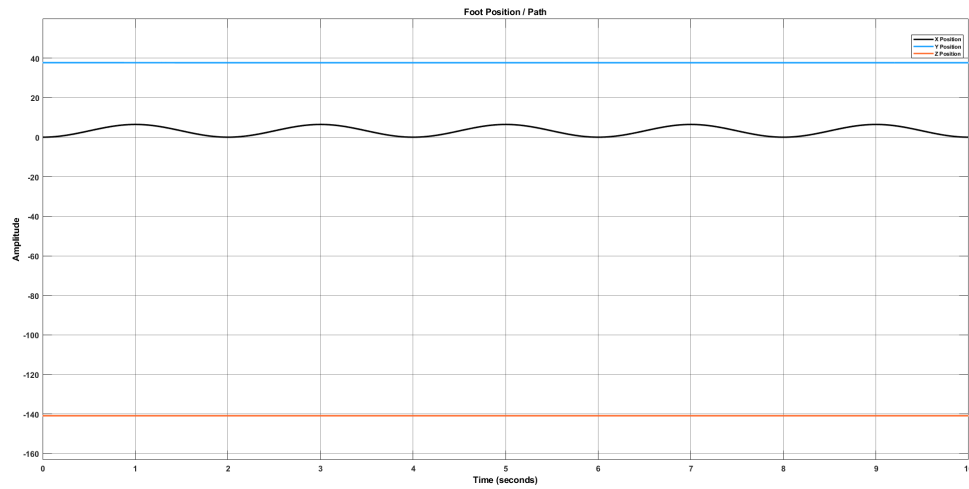


Figure 8: Foot Position

3.5 Foot Velocity

In figure 9 the trajectory of the foot over time concerning the three axes of the base frame while aiming for a sinusoidal speed specifically along the X-axis. The graph demonstrates the path followed by the foot in a timeframe concerning the movement along the X, Y, and Z axes of the base frame.

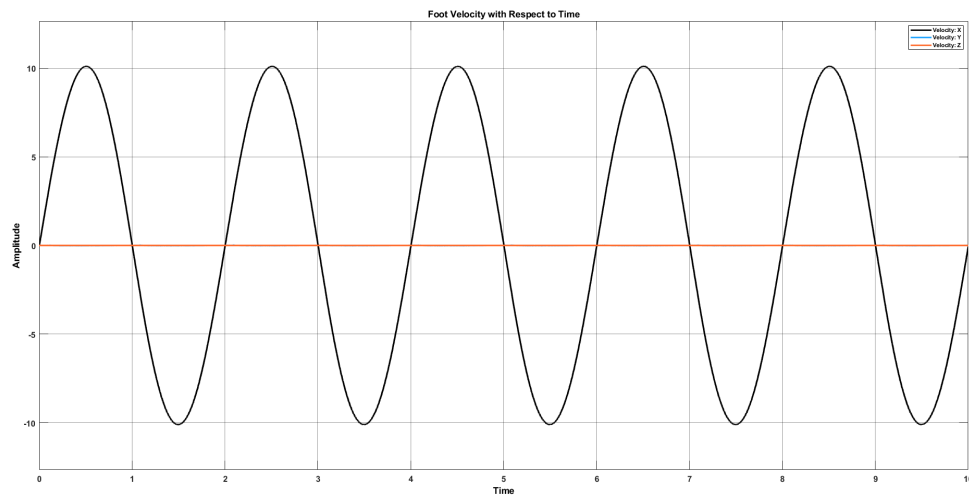


Figure 9: Foot Position

3.6 Comparative Analysis between Input and Velocity

Input Data: The input data in this figure represents the commands given to the hexabot leg. These commands has desired positions to control the leg's motion.

Velocity Data: The velocity data represents the rate at which the hexabot leg moves in response to the input commands. It shows how fast the leg is changing its position or orientation in different directions. From the figure we can see both of the input and output graph align with each other with the same amplitude.

Furthermore, the magnitude of the velocity along the X-axis distinctly aligns with the amplitude of the input sinusoidal signal, maintaining a constant factor of 10. This observation reinforces that the velocity output is directly proportional to the input signal's amplitude, exclusively influencing and resulting in a tenfold amplitude specifically along the X-axis. The figure visually highlights the sole influence of the input signal on the X-axis velocity, showcasing a magnitude precisely amplified by a factor of 10.

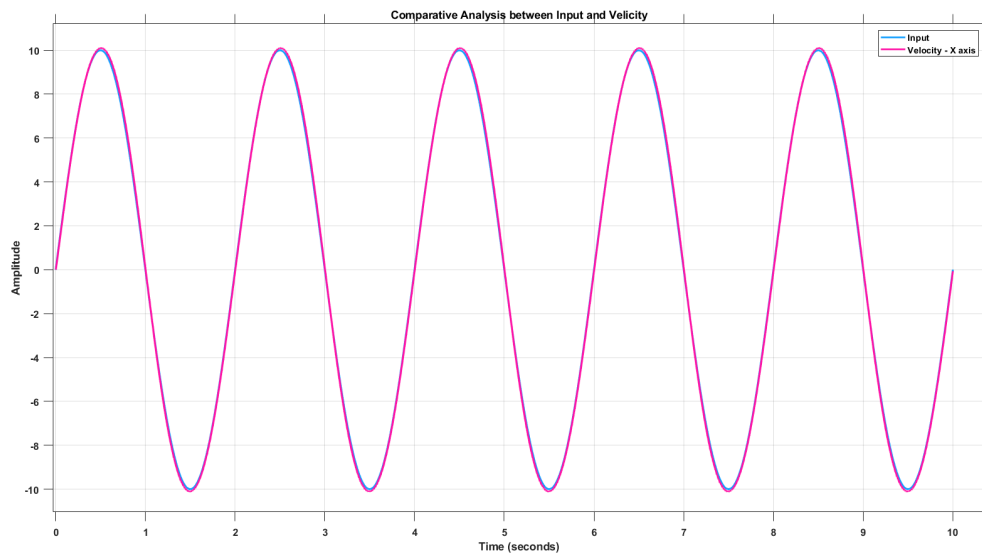


Figure 10: INPUT vs Velocity

3.7 Comparative Analysis between Velocity and Position

In Figure 11, the phase difference of 90 degrees between the position and velocity curves. This disparity in phase alignment is a direct consequence of differentiation: the velocity represents the rate of change of position. Therefore, when differentiating the position data to obtain velocity, a phase shift becomes evident in the velocity versus position graph. As differentiation calculates the rate of change, the velocity graph—being the derivative of the position graph—reflects this phase difference, resulting in a quarter-cycle (90 degrees) phase shift between the two curves. This discrepancy in phase between the position and velocity graphs is a fundamental outcome of differentiation, emphasizing the temporal shift inherent in the relationship between position and its derivative, velocity.

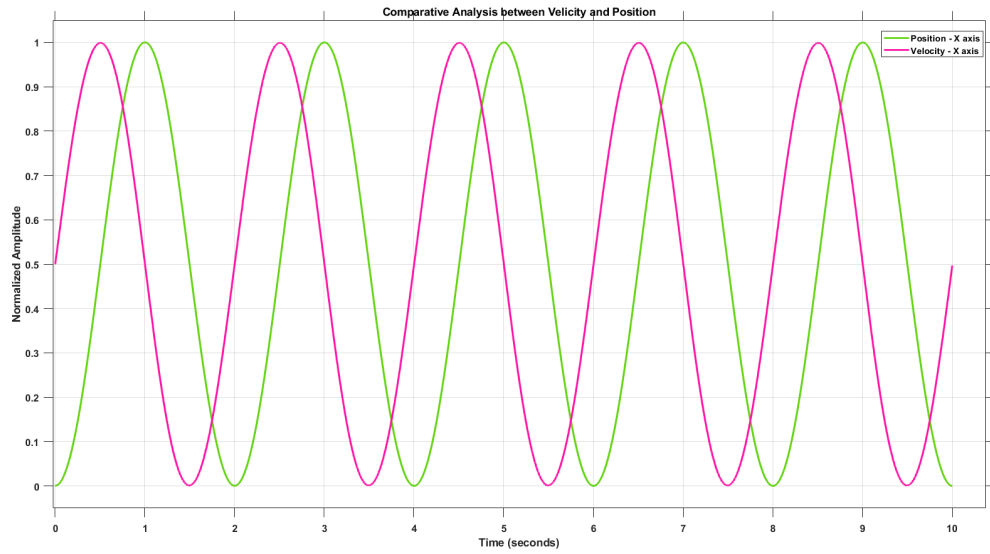


Figure 11: Velocity and Position

3.8 Comparative Analysis between Input, Velocity and Position

This graph illustrates the behavior of the model during forward motion. It shows that the input velocity and position are synchronized with the output velocity, resulting in a motion pattern where the model's behavior is aligned with the expected forward movement.

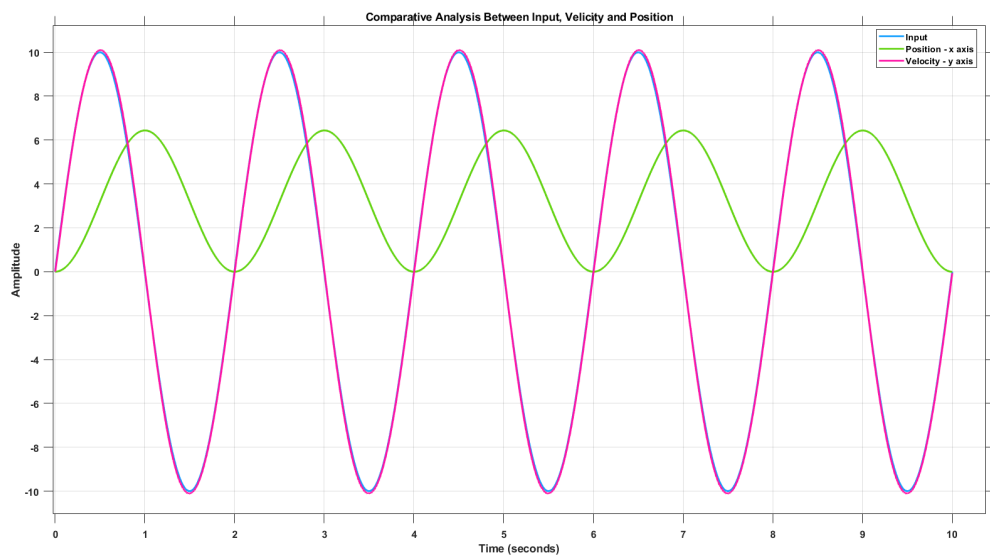


Figure 12: INPUT vs Velocity and Position